Identification and Localization of non-zero Resistance Short circuit Faults in Distribution Feeders Based on the Theory of Wavelets and Artificial Intelligence

Sara J. Authafa
Power and Machines Dept
College of Engineering
University of Basra
saraauthafa7@gmail.com

Khalid M. Abdul-Hassan
Power and Machines Dept.
College of Engineering
University of Basra
khmh7447@gmail.com

Abstract: **This paper introduces a radial distribution feeder protection scheme based on certain features extraction from current signals measurement at the substation. The features are captured using the discrete wavelet transform (DWT). Two digital signals processing methods are used to introduce those features to the 1) fault detection 2) identification and 3) localization schemes; the first one is the energy method and the second one is the root mean square method. For the purpose of fault type identification, two systems are tested and compared, a Fuzzy Inference System (FIS) and Artificial Neural Network (ANN). Fault location scheme is then built based on ANNs. An effort is made to reduce the computational burden and the speed of detection provided by the fault detection and identification schemes. Since the short circuit faults are the most likely types of faults that can occur in power systems, the ten types of these faults taking into account different fault resistances are simulated in MATLAB environment and the protection scheme is built based on the idea of over current. The power quality disturbances such as switching transient events on the feeder is also taken into account in order to build a reliable and secure protection scheme.**

Index Terms: **Distribution Feeder, Wavelets, Fault Detection, Fault Location, Cascade Neural Networks, Fuzzy Inference System**

I. INTRODUCTION

Distribution systems constitute the final stage of power delivery to consumers. Their conductors can be of overhead or underground types or a mixture of the two. Owing to the exposure to the natural environment, the overhead distribution feeders are usually more prone to external fault causes such as rain, wind, lightning and interference with objects like trees and vehicles. Fault causes can also be internal such as insulation degradation and failure. The formation of a conducting path between phase conductors and ground or between one another can cause a flow of a dangerously high amounts of currents that stress and damage the system components and may provide risk to human lives. The presence of such problems has led to the proposal of various fault detection, type and location techniques in an effort to reduce fault risk circumstances. the use of wavelet analysis provides the analysts a powerful tool for improving the old fault identification techniques by applying it as a pre-processing analysis tool. Wavelet transform introduces fast response, cost effectiveness and accuracy. A lot of the researches work made use of wavelet transform at higher stages where fault signatures can be more significant.

The choice of the most desirable stage differs from one application to another and from one mother wavelet to another, it also depends on the length of the signal to be analysed. The large number of decompositions, filter length and the nature of the extracted feature can increase the time required by fault detection and classification systems [1]. Accurate fault analysis and system response have to introduce more time for the relaying process. Building a scheme for which good accuracy as well as fast response is desirable to improve digital relaying functionality. A lot of research papers has been introduced in this field. A study of fault features curried by voltage signals at the load end of a transmission line is presented in [2]. The detail and approximation coefficients extracted by the db4 mother wavelet filter at the level4 of decomposition stages reveals significant trends of voltage signals at the time of fault initiation, similar trends can be found in current signals measured at the substation at the same fault type circumstances. Such effects are the result of short circuit faults by which abrupt changes in the current signals usually take place. These characteristics have been utilized by many fault detection and classification studies; however Many of the mentioned studies involved transmission power systems. Application of such techniques on distribution systems may require certain modifications to adapt with their complex nature such as non-homogeneity, the presence of loads, laterals and power quality disturbances. The reviewed fault type indication techniques are based mostly on artificial intelligence methods such as FIS [3]-[4] and an ANN [2], [5]-[9]. As regard to fault location techniques, four methods are usually introduced; these methods can be travelling wave based [10]-[11], impedance [12]-[13], ranking analysis according to a previously stored database [14]-[15], or artificial intelligence based [8], [16]-[19]. It can be seen that intelligent based techniques such as fuzzy, neural, genetic algorithms. etc. are dominating the field studies in the last few years. Their attributes of less complexity, better accuracy and faster response give them superiority over old complex techniques.

In this paper, the proposed scheme is divided into three parts, the first part is the detection scheme that is based on the wavelet analysis of a specific function along with the utilization of the moving frame signal processing technique to improve the speed of detection. The second and the third parts are the fault type classification and the fault localization schemes respectively. The effect of fault resistance that maybe encountered by the flow of short circuit current is considered in the analysis in order to account for the soil resistance of the ground path or the possibility of non-zero resistance objects existence between conductors during faults.

II. A GENERAL OVERVIEW OF WAVELET ANALYSIS

In power system fault analysis, it is important to detect certain trends in the signals to be analyzed to improve the detection procedures. Wavelet transform (WT) has proven to be the best choice for fault identification techniques; wherein, a variable windowing technique is utilized to analyze nonstationary signals (having localized changes which is the dominant behavior of faulty signals). In this technique, accuracies in both time and frequency can be gained as compared to short time Fourier transform (STFT) that has one fixed resolution in time and frequency which is regarded as a drawback.

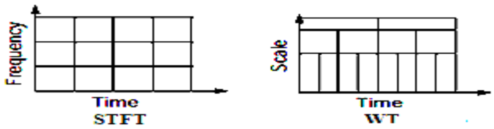

Fig. 1 Differences between Fourier transform (STFT) and wavelet transform (WT)

The major advantage of this type of the analysis, is its capability in revealing aspects like trends, breakdown points and discontinuities. the basis function used by Wavelet analysis is called wavelets, they are waveforms of finite duration with irregularity trends and an average value of zero. Their wave-shapes help in revealing local sharp changes that the sine waves cannot. There are several types of Wavelet transform that originated from a basic type called continuous wavelet transform (CWT). the CWT is defined as the sum over all time of the analyzed signal multiplied by shifted and scaled versions of the basis function (Wavelet function Ψ) as follows :

$$\Psi(a,b) = a^{-1/2}\,\Psi(a^{-1}(t - b)) \qquad (1)$$

$$C(a,b) = {}_{-\infty}\!\int^{+\infty} f(t)\, a^{-1/2}\, \Psi(a^{-1}(t-b))\, dt \qquad (2)$$

Where, C: The coefficients that represent how closely the wavelet function is correlated with that part of the signal $f(t)$, a: scaling parameter, b: shifting parameter.

Since Any signal processing method performed in a computer using real world data must be accomplished on a discrete signal, and since calculating CWT provides redundancy of values because of the small shifting and dilating steps, the choice of a finite number of scale and position steps based on a power of 2 (dyadic steps) has been introduced as follows :

$$a = 2^{j}, b = \mu\, 2^{j},\; W(j, \mu) = \Sigma\, k\, f(k)\, 2^{-j/2}\, \Psi(2^{-j} k - \mu) \qquad (3)$$

Where, $W(j, \mu)$: The DWT coefficients as a function of the new scaling and shifting parameters (j) and (μ). k: discrete time steps.

This approach is called the discrete wavelet transform (DWT) and can be realized using a set of filters into which the signal is passed and out of which the coefficients are emerged. Multi Resolution Analysis (MRA), is the iterative process of decomposing the analyzed signal by the DWT filters into approximation and detail components. Approximations represents low frequency components of the signal whereas details represent high frequency components. The signal that enters the DWT filters will be decomposed according to the MRA as shown in Fig. 2.

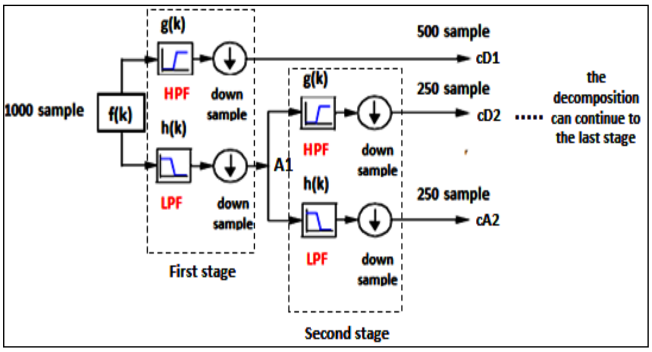

Fig. 2 DWT analysis

Where, cA: Approximation coefficients, cD: Detail coefficients, h(k), g(k) : represents the low and high pass filter coefficients respectively.

The structure reveals that the signal after being convolved with filters is down sampled by 2 in order to avoid duplication of the samples at each stage. The result is equal amount of samples as that of input signal. The frequency division of the signal by an MRA analysis is shown in Fig. 3. The first decomposition stage will divide the signal in frequency domain into two halves, the second stage will further decompose the first stage approximations frequency range into two halves and so on:

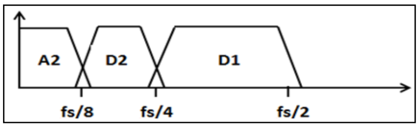

Fig. 3 Frequency band division by the DWT

Where, fs: The sampling frequency that satisfies Nyquist's sampling criteria which will be explained in detail in a later section. A1: first stage approximations, D1: first stage details.

III- Distribution Feeder Model

In order to perform fault test cases, MATLAB SimPowerSystems toolbox is usually utilized such that large power systems can be simulated accurately and measurement signals can be captured for the sake of storage and analysis. The general model of any feeder system is as shown in Fig. 4 where the loads can be localized at the end of the feeder or at specific tap points along the feeder length. The equivalent circuit models for the three phase transformer, line conductors, and loads are provided within the toolbox. Since the electrical model of the three phase distribution line is dependent on its phase impedance and shunt admittance matrices as shown in Fig. 5, these matrices has to be computed in order to substitute for their values throughout the equivalent MATLAB model for the line. The computations are dependent on Carson's equations utilizing the geometric data of the line as given in [20]. The test feeder is of overhead radial type and its topology is provided in Fig. 6. Because the shunt admittances in overhead short distribution feeders can be neglected [20], the series impedance matrix only is required for simulating short and overhead type distribution feeders. The system data required to build the equivalent simulation model are provided in the appendix, where the parameters of the line are computed and provided in [21]. The feeder simulation model is provided in Fig. 7. A number of switches are provided in the model to test for the various switching transient events. A bank of power factor improving capacitors were introduced at node 20 to test for the oscillatory transient events. A test for the harmonics provided by an energization of a no loaded transformer is also introduced by means of an equivalent model that is available within the toolbox for simulating such situation.

IV. Digital Signal Processing Requirements

In order to build a fast and reliable fault detection and identification scheme, the following considerations must to be taken into account:

A. Sampling Frequency

According to the Nyquist's sampling theorem, for a correct representation of a signal in the discrete state, the sampling frequency (fs) has to be equal to or larger than double the highest frequency content of the signal. The bandwidth of fault transient frequencies is usually between 0.1Hz -1 kHz, therefore fs has to be larger than or equal to 2 kHz [22]. For accuracy purposes fs is chosen to be 12.8 kHz and is calculated as follows:

The number of samples per cycle must be of a power of 2 which is a requirement of wavelet transform, the chosen number of samples per cycle is 256. As a result, fs will be equal to the fundamental frequency of the signal (50 Hz) multiplied by 256 which will give 12.8 kHz [23].

B. Frame Size

The frame size at which discretised current signals will be analysed is chosen to be of a quarter of cycle length, i.e. of 64 samples.

C. Choosing the Suitable Mother Wavelet

By applying a test on a number of faulty and healthy signals, the best mother wavelet for the analysis can be found [24]. A simple routine for the test is built within MATLAB m-file. The test is done using a set of Deaubichies mother wavelets of orders ranging from 2-10 (of respective filter lengths of 4-20). The flow chart of the method is shown in Fig. 8. The error between the original and the reconstructed signal is measured by the norm formula given in (4). The resultant mother wavelet is the one having the least error value.

$$norm(e) = \left(\sum_{K=1}^{N} (S_k - \hat{S}_k)^2\right)^{1/2} \quad (4)$$

Where, S: The original signal, $\hat{S}$: the reconstructed signal, k: The individual signal sample number, N: the length of signal. The test results shown in Table I reveal that the best choice is the Db2 mother wavelet.

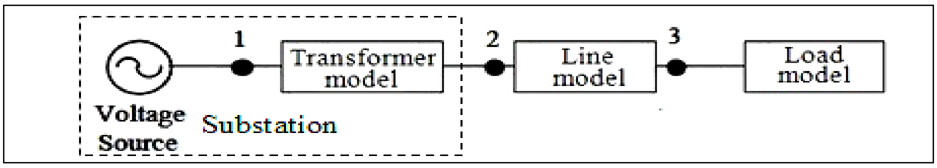

Fig. 4 Feeder system general model

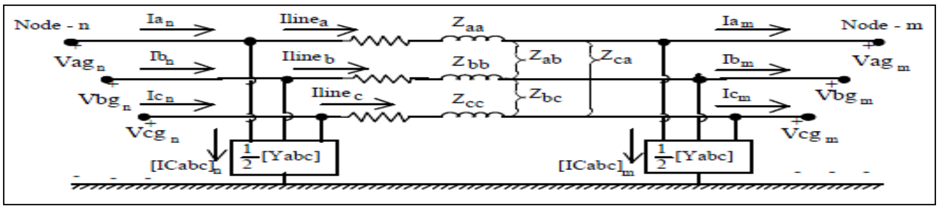

Fig. 5 Feeder line electrical model

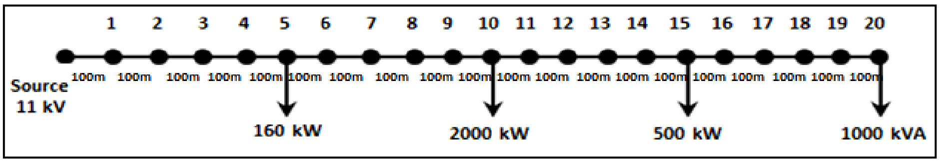

Fig. 6 Feeder Topology

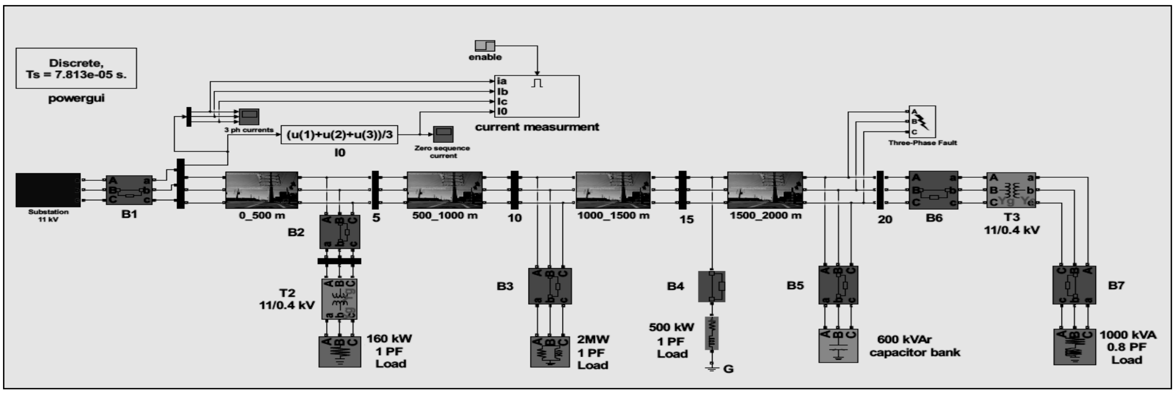

Fig. 7 Feeder simulation model

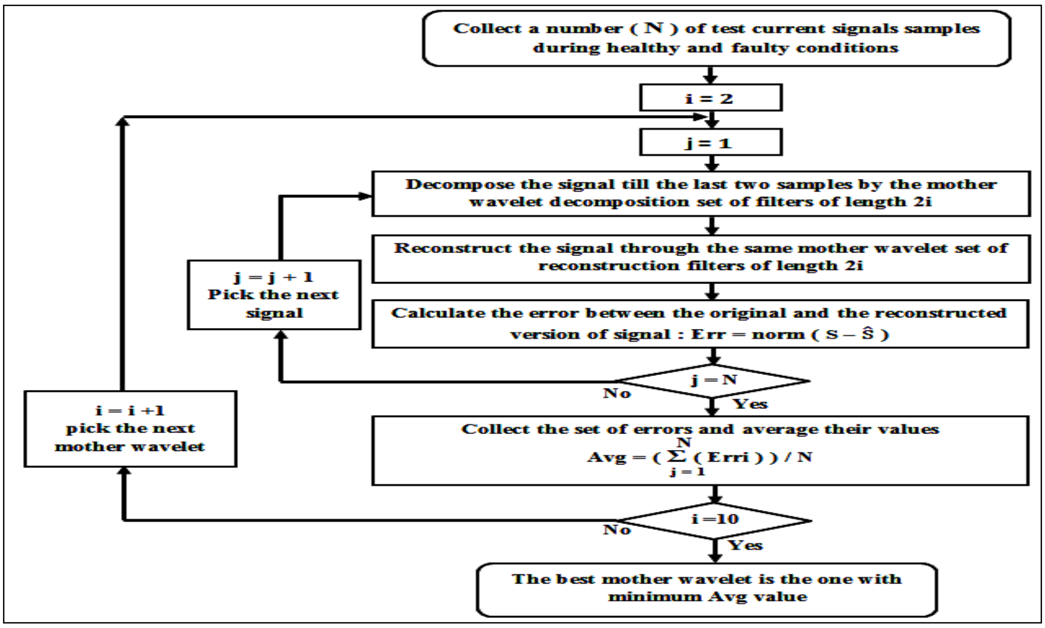

Fig. 8. Best mother wavelet test flow chart

TABLE I
AVERAGE ERROR VALUES FOR A COLLECTION OF DEAUBICHIES MOTHER WAVELETS

Db2	Db3	Db4	Db5	Db6	Db7	Db8	Db9	Db10
1.284e-08	1.399e-07	2.443e-08	3.764e-08	2.217e-08	2.454e-08	5.720e-08	3.827e-07	6.506e-08

D. Framing Technique

Since the framing of samples can increase or decrease the processing speed. The moving frame method is used in this work to fasten the detection speed to the least possible amount of time. This method is based on entering one sample at a time to the analysis window (the frame) and at the same time leaving one sample behind and so forth as shown in Fig. 9. As a result of introducing this technique, the speed of detection has been improved widely as shown in Figs. 10 & 11 for which the fault detection speed for a 15 Ohm 725 m far from source fault is simulated.

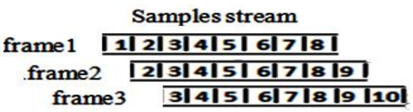

Fig. 9 The moving frame technique representation of samples

E. Signal Features Representation

1) *Energy of Samples*:

$$E = \sum_{i=1}^{N} | S_i |^2 \quad (5)$$

2) *RMS of Samples* [25]:

$$S_{RMS} = \left(\sum_{i=1}^{N} | S_i |^2 \right)^{1/2} \quad (6)$$

Where, S_i: Signal samples

F. Signals Specifications during healthy and Faulty conditions

It is found that during healthy conditions, the signals detail and approximation coefficient values are within normal limits. The detail and approximation coefficients are having small values as compared to faulty situations. These trends can be utilized to detect, classify and localize faults. An example of such changes in signals extracted features is shown in Fig. 12.

V. THE PROPOSED FEEDER PROTECTION SCHEME

The protection algorithm is dependent on three sequential phases, which are:

A. The Fault Detection Phase

The requirement of a detection scheme has led to the utilization of a certain function to reduce computational demands and detection time due to its concentration effects of fault transients [1], this function is given in (7):

$$f[n] = (a[n]^2 + b[n]^2 + c[n]^2)^{1/2} \quad (7)$$

According to the tests, it is found that the major sources of Transient events that can affect the detection procedure during healthy conditions are the switching transients, such as the energization of a capacitor bank, a no loaded transformer or the main feeder. As a result, by DWT decomposing the mentioned function to the first level details and approximations by Db2 filters, the healthy system condition can be distinguished from faulty one overcoming such disturbances. The analysis performed on f[n] is provided in Fig. 13. The flow chart of the fault detection procedure is shown in Fig. 14. The values of the thresholds mentioned in the figures are as follows:

For Energy method: Threshold1 =3.3e+7; Threshold2 =33
For RMS method: Threshold1 =1000; Threshold2 =1

B. Fault Type Classification phase

Two systems are tested and compared to identify fault types, the first one utilizes a fuzzy inference system (FIS) and the second utilizes an artificial neural network (ANN).

The flow chart of the fault type classification scheme is provided in Fig. 15.

1) FIS Application

A Mamdani type FIS is chosen to classify fault types. In order to build the system, the following points must be taken into account:

- The inputs must be chosen based on observations of the relationships between healthy and faulty phase current samples DWT extracted features.
- The chosen features must be manipulated by certain processing functions to facilitate the classification procedure.
- The sample space of inputs and output must cover the all possible values.
- Membership function shapes and ranges must be decided.
- The rules are formulated based on the behaviour of input features with related outputs for different fault types.

The inputs are chosen to be the normalized energy or RMS representation of detail components of current samples, the resultant are 4 inputs. The inputs processing is shown in Fig. 16 where Db2 is chosen for the DWT. The system structure, membership functions, specifications and rules are provided in Figs. 17, 18, 19 and Tables II and III respectively.

2) *ANN application*:

A cascade forward NN is used to represent fault type. This type of network is a feedforward net with additional weight connections between layers, adding them will improve the network performance. Simulation data is provided for various fault cases regarding different nodes of the feeder and different fault resistances ranging from 0 to 20 Ohm. To build the network the following points must be followed:

- Choose the features to be extracted from the current signals and feed it to the ANN.
- The provided data for the network must be divided into training, validation and test sets. A specific neural network toolbox built-in function called divide random is used such that the provided set of simulated fault cases extracted features are divided randomly to 80% training and 20% validation data with an individual set is provided to test for the network generalization.
- The inputs will be pre-processed by another built-in functions such as map min-max that transforms input data such that all their values will fall in the interval [-1,1], the other function is remove constant rows that removes duplicated input values. The targets will have the same processing functions in order to transform the provided targets to useful values for the network use, after that the network outputs will be reverse processed to provide the same user provided output data. The provision of such functions is to improve network learning capabilities.
- Decide the number of neurons and the structure of the hidden layer.
- Train the network by a chosen training function to have the least mean squared error (MSE). Levenberg Marquardt (trainlm) and Bayzian regularization (trainbr) training functions has been tested for the energy and RMS types of inputs.

After performing a number of tests, the ANN input features are chosen as the first stage analyzed current samples Db2 related details and approximations represented by an energy once and RMS second as. As a result, the ANN will have 8 inputs. The ANN input calculations is shown in Fig. 20, the specifications of the tested ANNs are provided in Table IV.

C. The Fault Localization Phase

A modular type ANN of cascade forward nets is used for determining fault locations. The Fault types are divided into four classes, for each class an individual fault location ANN is used. For this arrangement, the network performance can be improved greatly. The same inputs of fault type ANN described in the fault type classification phase are used for fault localization procedure. The flow chart of the fault location process is shown in Fig. 21, the specifications and the tested ANNs are provided in Table V.

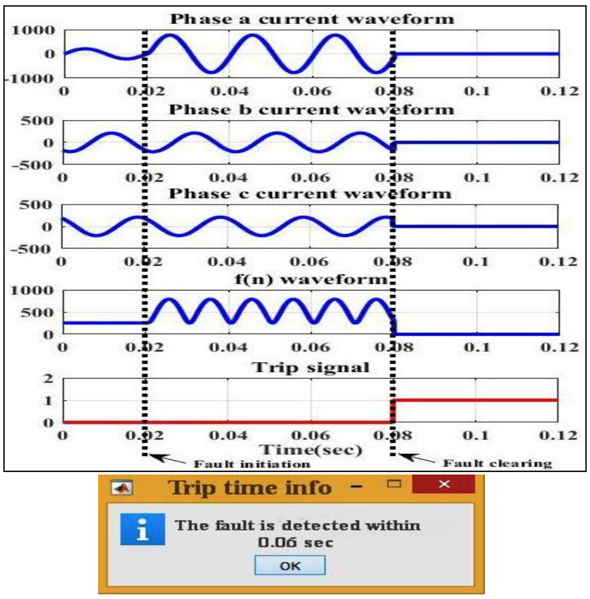

Fig. 10 The Fault detection for the regular framing technique

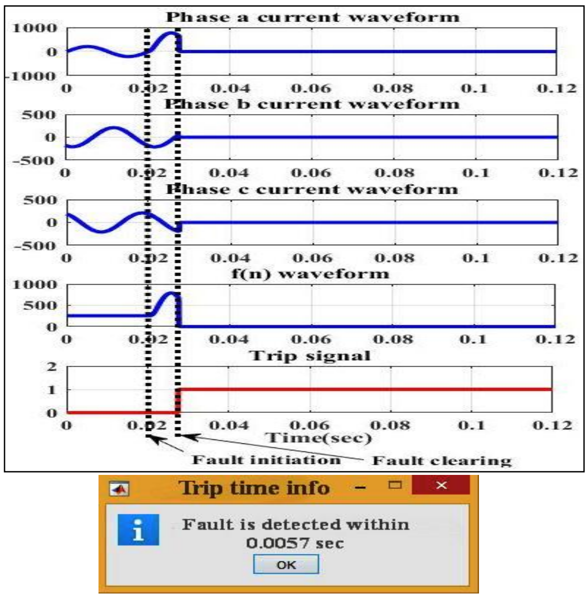

Fig. 11 The Fault detection for the moving frame technique

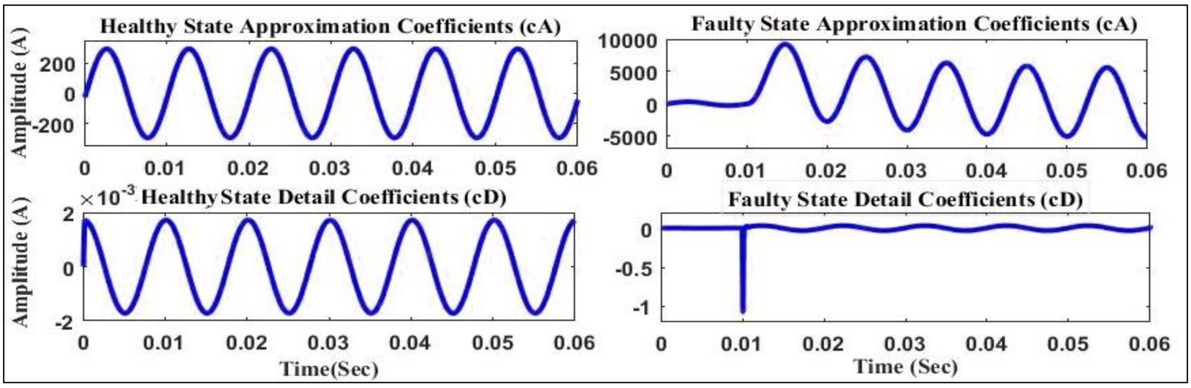

Fig. 12 DWT related first stage db2 decomposition coefficients during healthy and faulty conditions

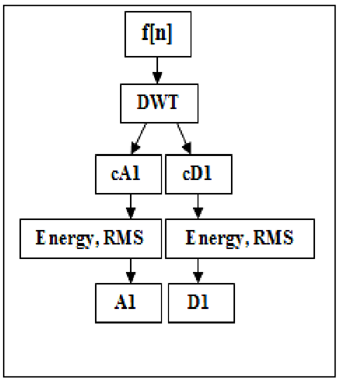

Fig. 13 f[n] analysis structure

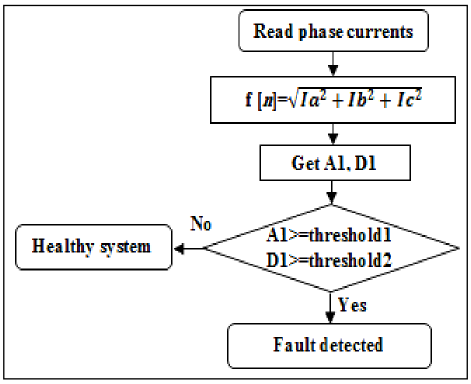

Fig. 14 A flowchart for the fault detection procedure

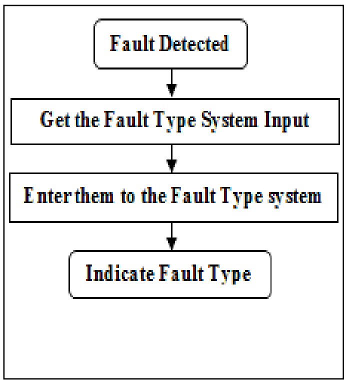

Fig. 15 Fault type identification flow chart

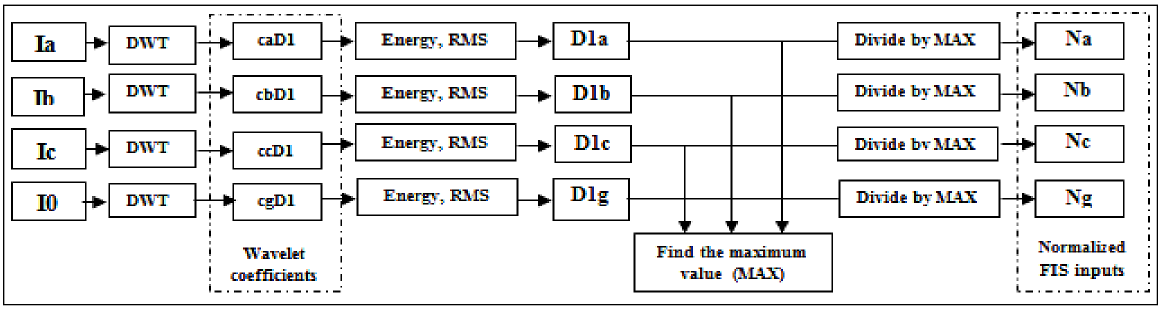

Fig. 16 FIS inputs calculations

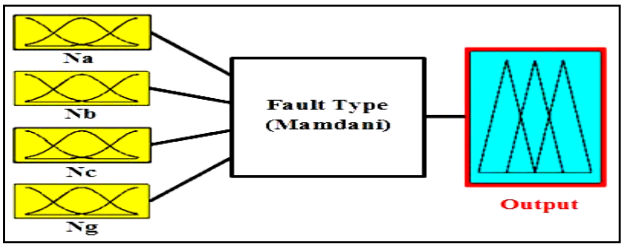

Fig. 17 FIS structure

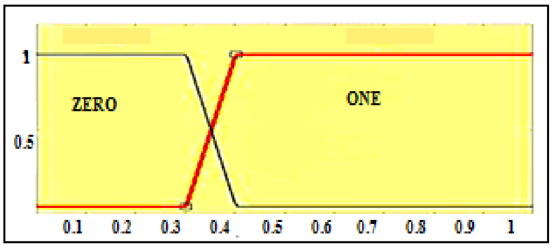

Fig. 18 An input variable membership functions

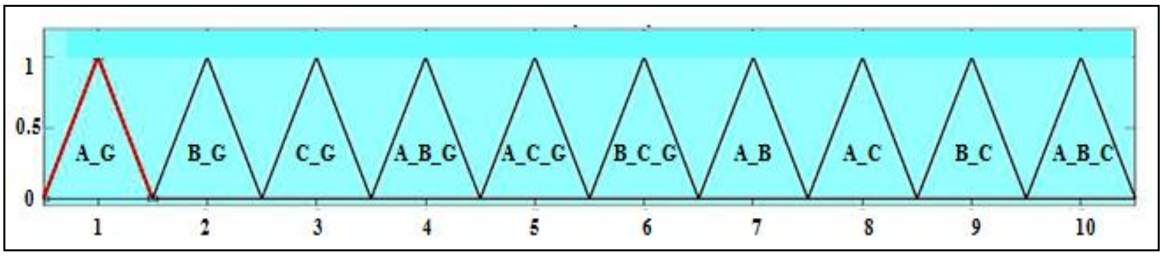

Fig. 19 Output variable membership functions

TABLE II
FIS SPECIFICATIONS

Input Variable Membership Functions	**Na, Nb, Nc**					**Ng**			
	Mf Type	**No. of Mfs**	**Names**	**Range**	**Parameters**	**No. of Mfs**	**Names**	**Range**	**Parameters**
	Trapezoidal Mf	**2**	**Zero**	0-0.4	0,0,0.35,0.4	2	**Zero**	0-0.01	0,0,0.008,0.01
			One	0.35-1	0.35,0.4,1,1		**One**	0.008-1	0.008,0.01,1,1
Output Variable Membership Functions	**Type**	**No. of Mfs**	**Names**	**Range**	**Parameters**				
	Triangular Mf	**10**	**A-G**	0-1.5	0, 1, 1.5				
			B-G	1.5-2.5	1.5, 1, 2.5				
			C-G	2.5-3.5	2.5, 2, 3.5				
			AB-G	3.5-4.5	3.5, 4, 4.5				
			AC-G	4.5-5.5	4.5, 5, 5.5				
			BC-G	5.5-6.5	5.5, 6, 6.5				
			AB	6.5-7.5	6.5, 7, 7.5				
			AC	7.5-8.5	7.5, 8, 8.5				
			BC	8.5-9.5	8.5, 9, 9.5				
			ABC	9.5-10.5	9.5, 10, 10.5				
AND method	**Min**								
Implication	**Min**								
Aggregation	**Max**								
Deffuzification	**Centroid**								

TABLE III
FIS RULES

Antecedent	**Consequent**
If Na is One AND Nb is Zero AND Nc is Zero AND Ng is One	**A_G**
If Na is Zero AND Nb is One AND Nc is Zero AND Ng is One	**B_G**
If Na is Zero AND Nb is Zero AND Nc is One AND Ng is One	**C_G**
If Na is One AND Nb is One AND Nc is Zero AND Ng is One	**A_B_G**
If Na is One AND Nb is Zero AND Nc is One AND Ng is One	**A_C_G**
If Na is Zero AND Nb is One AND Nc is One AND Ng is One	**B_C_G**
If Na is One AND Nb is One AND Nc is Zero AND Ng is Zero	**A_B**
If Na is One AND Nb is Zero AND Nc is One AND Ng is Zero	**A_C**
If Na is Zero AND Nb is One AND Nc is One AND Ng is Zero	**B_C**
If Na is One AND Nb is One AND Nc is One AND Ng is Zero	**A_B_C**

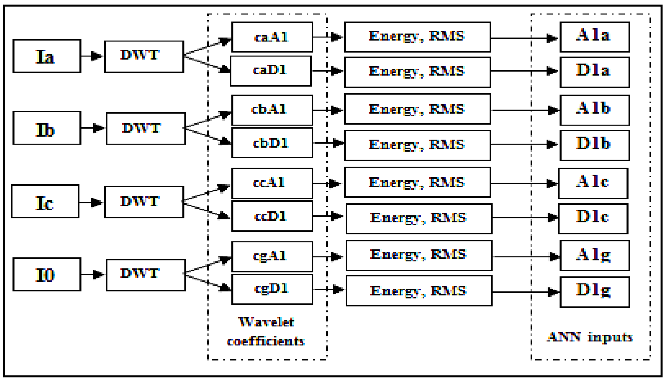

Fig. 20 ANN Fault type input calculations

TABLE IV
FAULT TYPE ANN SPECIFICATIONS AND A COMPARISON BETWEEN DIFFERENT ANNS HAVING DIFFERENT TRAINING FUNCTIONS AND INPUT TYPES

Type of ANN	**Cascade forward net**			
No. of hidden neurons	**25**			
Network structure	**8-20-5-1**			
Hidden layer transfer function	**Tan sigmoid**			
Output layer transfer function	**Linear**			
Training method	**Backpropagation training**			
Performance function	**Mean squared error (MSE)**			
Testing various training functions & input types	**Energy inputs**		**RMS inputs**	
	Trainlm	**Trainbr**	**Trainlm**	**Trainbr**
training performance	**4e-4**	**7e-4**	**1e-4**	**1.4e-3**
Best validation performance	**7e-4**	**9.8e-4**	**1.3e-4**	**1.5e-3**
Test performance	**3.26e-4**	**5.5e-4**	**5.9e-5**	**8.6e-4**
Training regression	**0.99997**	**0.99996**	**0.99999**	**0.99992**
Validation regression	**0.99995**	**0.99993**	**0.99997**	**0.9999**
Epochs	**449**	**346**	**162**	**431**

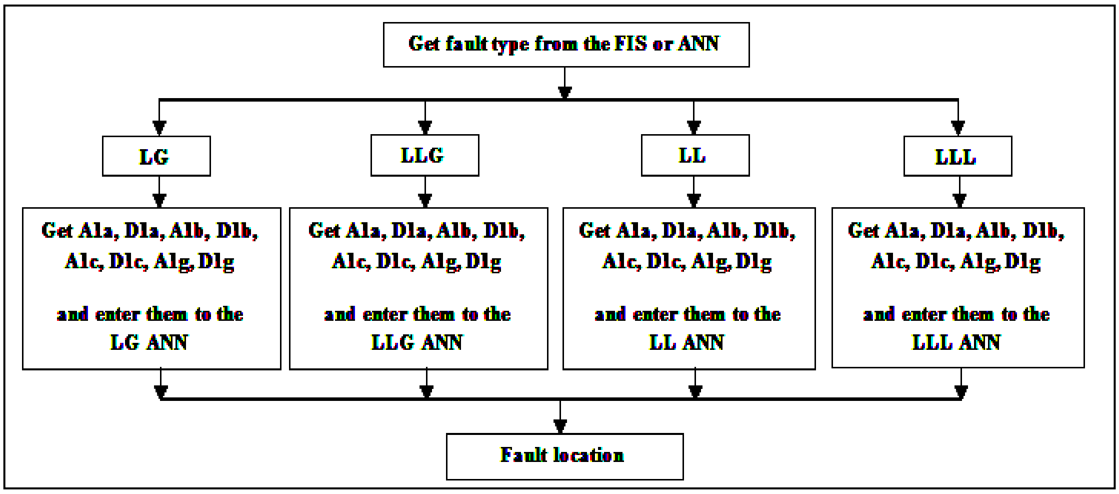

Fig. 21 ANN Fault location indication flow chart

TABLE V
FAULT LOCATION ANNS SPECIFICATIONS AND A COMPARISON BETWEEN THE DIFFERENT ANNS HAVING DIFFERENT TRAINING FUNCTIONS AND INPUT TYPES

Type of ANNs	**Cascade forward net**				
Hidden layer transfer function	**Tan sigmoid**				
Output layer transfer function	**Linear**				
Performance function	**Mean squared error (MSE)**				
LG ANN	**No. of hidden neurons**	**48**			
	Network structure	**8-8-16-16-8-1**			
	Testing various training functions & input types	**Energy**		**RMS**	
		Trainlm	**Trainbr**	**Trainlm**	**Trainbr**
	training performance	**1e-2**	**1e-2**	**1e-2**	**1e-2**
	Best validation performance	**1.16e-2**	**1.105e-2**	**1.169e-2**	**1.47e-2**
	Test performance	**0.0101**	**0.0103**	**0.0115**	**0.0111**
	Epochs	**988**	**1257**	**862**	**596**
	Training regression	**0.9999**	**0.9999**	**0.9999**	**0.9998**
	Validation regression	**0.9998**	**0.9998**	**0.9997**	**0.9997**
LLG ANN	**No. of hidden neurons**	**56**			
	Network structure	**8-8-16-16-16-1**			
	Testing various training functions & input types	**Energy**		**RMS**	
		Trainlm	**Trainbr**	**Trainlm**	**Trainbr**
	Training performance	**1e-1**	**1e-2**	**8e-3**	**5.4e-3**
	Best validation performance	**1.37e-2**	**1.04e-2**	**9.79e-3**	**7.24e-3**
	Test performance	**0.018**	**0.0112**	**0.0102**	**0.008**
	Epochs	**476**	**387**	**370**	**412**
	Training regression	**0.9998**	**0.99988**	**0.99988**	**0.9999**
	Validation regression	**0.9997**	**0.99984**	**0.99984**	**0.9998**
	No. of hidden neurons	**56**			
LL ANN	**Network structure**	**8-8-16-16-16-1**			
	Testing various training functions & input types	**Energy**		**RMS**	
		Trainlm	**Trainbr**	**Trainlm**	**Trainbr**
	Training performance	**1e-2**	**1e-2**	**4.6e-3**	**7.3e-3**
	Best validation performance	**1.3e-2**	**1.27e-2**	**9.75e-3**	**8.84e-3**
	Test performance	**0.019**	**0.0126**	**0.05**	**0.02**
	Epochs	**780**	**1558**	**346**	**227**
	Training regression	**0.9998**	**0.9999**	**0.9999**	**0.9998**
	Validation regression	**0.9998**	**0.9978**	**0.9998**	**0.9998**
LLL ANN	**No. of hidden neurons**	**34**			
	Network structure	**8-8-16-8-1**			
	Testing various training functions & input types	**Energy**		**RMS**	
		Trainlm	**Trainbr**	**Trainlm**	**Trainbr**
	Training performance	**8.5e-3**	**9.75e-3**	**9.97e-3**	**5.4e-3**
	Best validation performance	**1.7e-2**	**1.4e-2**	**2e-2**	**1.3e-2**
	Test performance	**0.018**	**0.03**	**0.025**	**0.028**
	Epochs	**297**	**303**	**135**	**146**
	Training regression	**0.99989**	**0.99985**	**0.99984**	**0.9999**
	Validation regression	**0.99956**	**0.99946**	**0.99918**	**0.9995**

VI. TEST RESULTS AND DISCUSSION

A Fault protection routine written in MATLAB environment is used to mimic digital relay processing functions. By running such program, the fault protection scheme can be tested. The test interval consists of 6 cycles, All the faults and sudden events are initiated at the second cycle from the interval. The fault type and location systems accuracies, comparisons between the systems involved, test cases on healthy and faulty conditions and speed of detection are introduced in this section. For the test cases, system condition is declared through an instant message box that contain information of the fault type and location in case of fault detection. Faults test cases have been taken at locations 725 m, 1250 m, 1575 m distant from source which are represented by L1, L2, and L3 respectively. The fault resistance is regarded as 5 Ohms. This yield about 30 test cases such that each test location will have 3 LG, 3 LLG, 3 LL, and 1 LLL fault test cases.

A. Fault Type

Testing the FIS with the energy normalized inputs once and RMS inputs second reveals the same results; on the other hand, the neural network with the least value of test performance is found to be the one with the energy inputs and trainlm training function as shown in Table IV. A comparison between the FIS and the mentioned ANN to verify which system is better to accurately classify fault types is introduced in Table VI, in which, the successful predictions out of 30 fault type systems test cases are shown. The results show the ability of the ANN to classify all fault types as compared to the FIS.

TABLE VI
A COMPARISON BETWEEN THE FIS AND ANN FAULT TYPE SYSTEMS ACCURACIES MEASURED BY THE NUMBER OF SUCCESSFUL PREDICTIONS OF TEST CASES

General Fault Types	FIS			ANN		
	L1	L2	L3	L1	L2	L3
LG	3	3	3	3	3	3
LLG	2	2	2	3	3	3
LL	3	3	3	3	3	3
LLL	1	0	0	1	1	1

B. Fault Location

Table V shows that for LG and LLL ANNs, the best networks according to the values of the test performances are those of energy inputs and trainlm training functions; whereas for LLG and LL faults, the best ones are those having trainbr training functions with RMS inputs for LLG and energy inputs of LL fault types. Since the energy input ANNs in fault type classification scheme and most of the fault location constituent ANNs are having the least values of test performances, these types of ANNs are chosen for the overall proposed scheme. Table VII shows the 30 test set cases fault location predictions error percentages calculated as given in (8) [13]:

$$Err\,\% = ((A - P) / Le) \text{ X } 100\ \% \qquad (8)$$

Where, A: the actual fault location, P: the predicted fault location, Le: total length of feeder.

TABLE VII
THE FAULT LOCATION SET OF ANNS PREDICTION RESULTS MEASURED BY THE PERCENTAGE OF ERROR

Fault location individual ANNs	Average (*Err%*)
LG _ANN (9 cases)	0.775%
LLG _ANN (9 cases)	0.74%
LL _ANN (9 cases)	0.13%
LLL _ANN (3 cases)	0.883%

C. Test Cases on Healthy and Faulty Conditions

1) Healthy States:

- *Normal Operation*

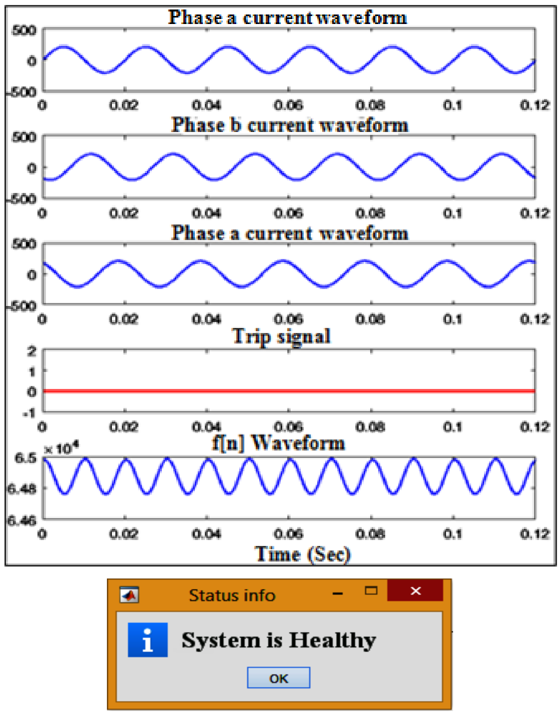

Fig. 22 Normal system operation

- *Capacitor Switching*

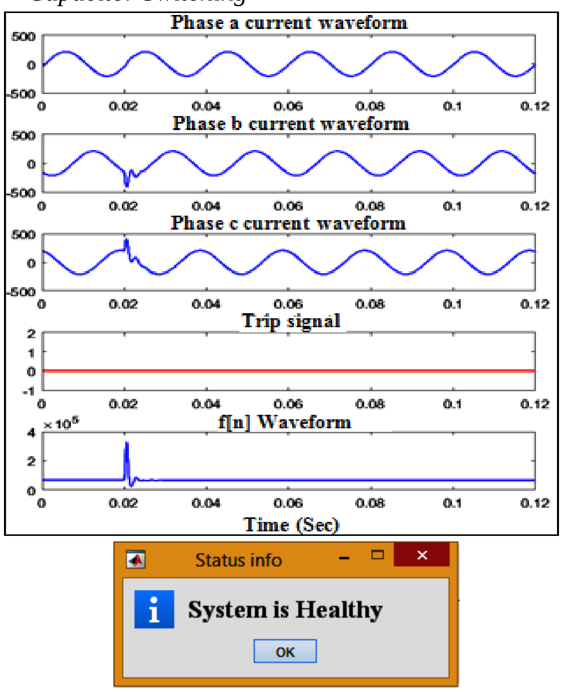

Fig. 23 Capacitor bank energization event

• *Transformer Energization*

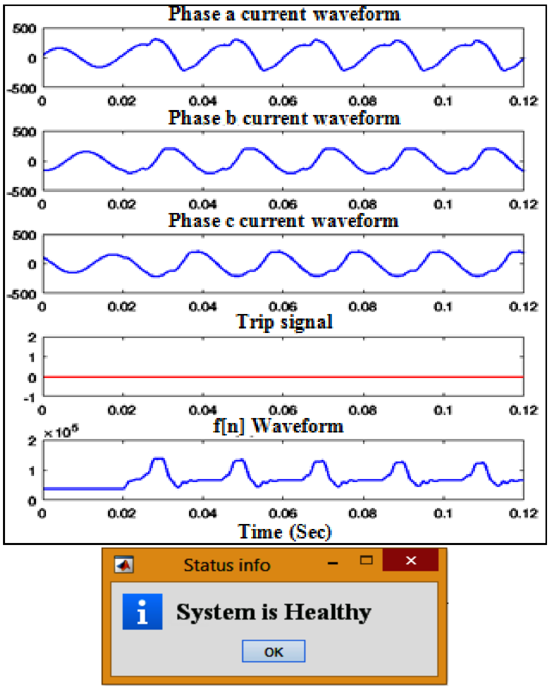

Fig. 24 An energization of a no loaded transformer

• *Energizing the Main Feeder*

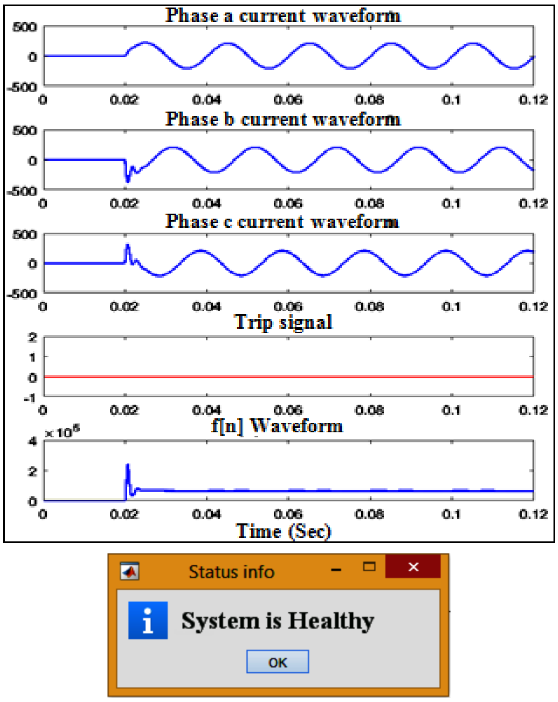

Fig. 25 An energization event of the main feeder

2) Faulty States:

The results of 12 fault cases simulated at locations L1, L2, and L3 with an Rf = 5 Ohms are shown in the following figures where the trip signal is initiated and the main substation circuit breaker is opened, then the fault type and location is declared in the respective message boxes.

• *A_G Fault at L1*

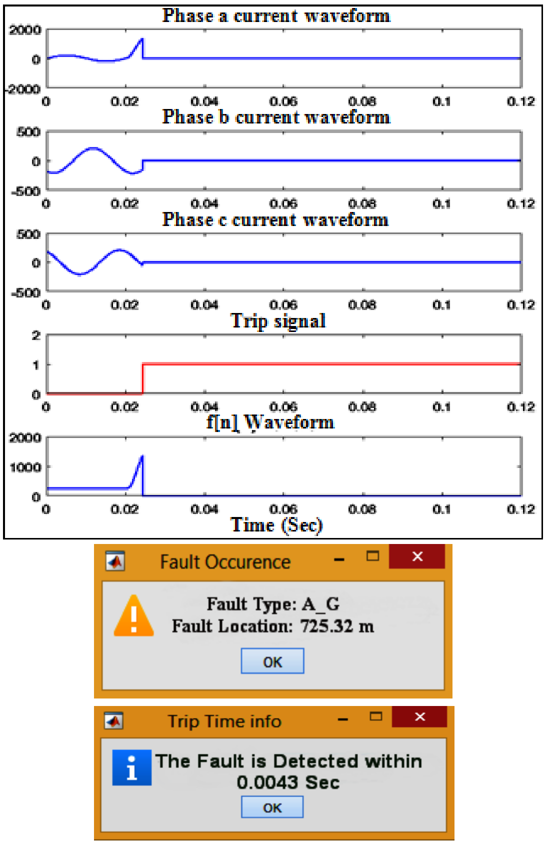

Fig. 26 A_G fault at L1

• *B_G Fault at L2*

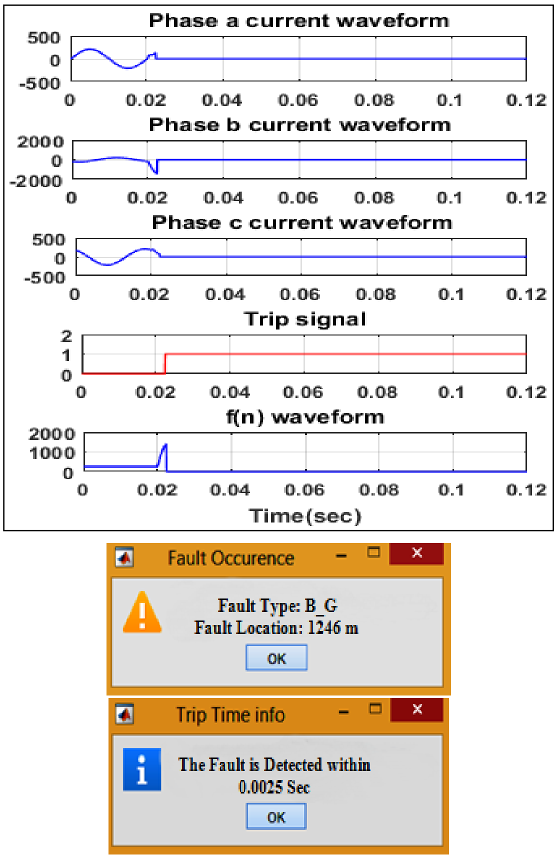

Fig. 27 B_G fault at L2

- *C_G Fault at L3*

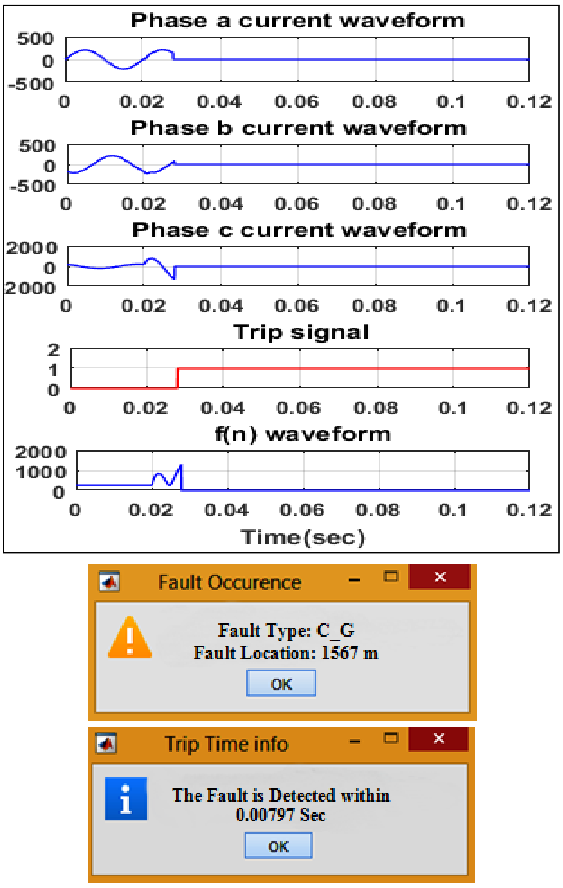

Fig. 28 C_G fault at L3

- *A_C_G fault at L2*

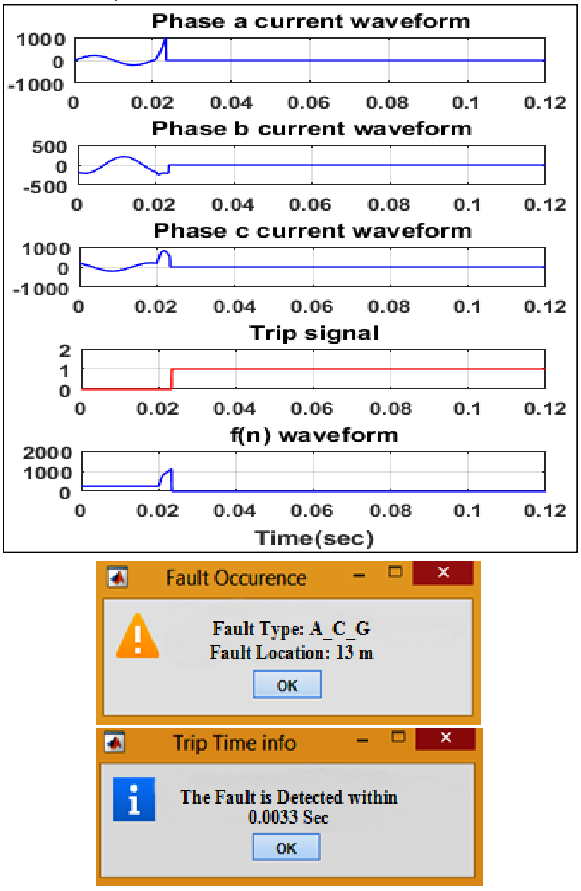

Fig. 30 A_C_G fault at L2

- *A_B_G Fault at L1*

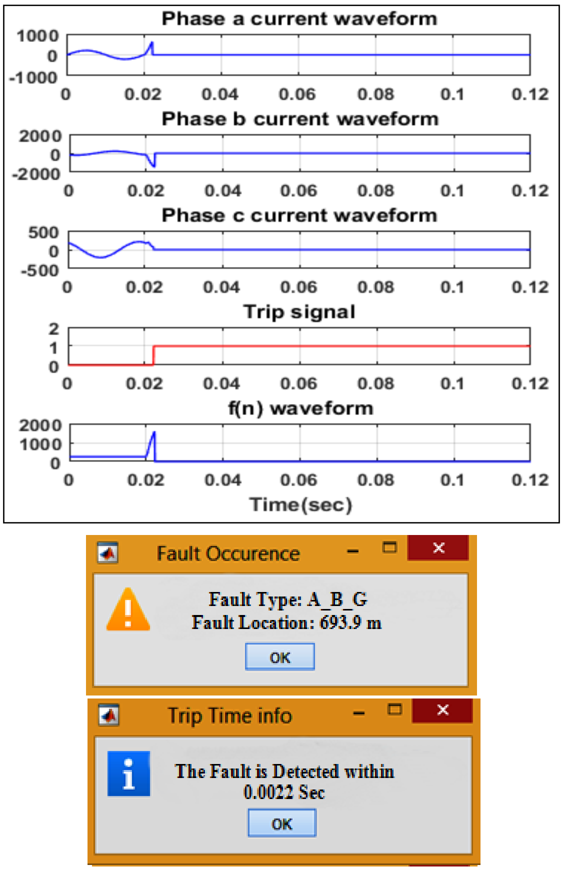

Fig. 29 A_B_G fault at L1

- *B_C_G Fault at L3*

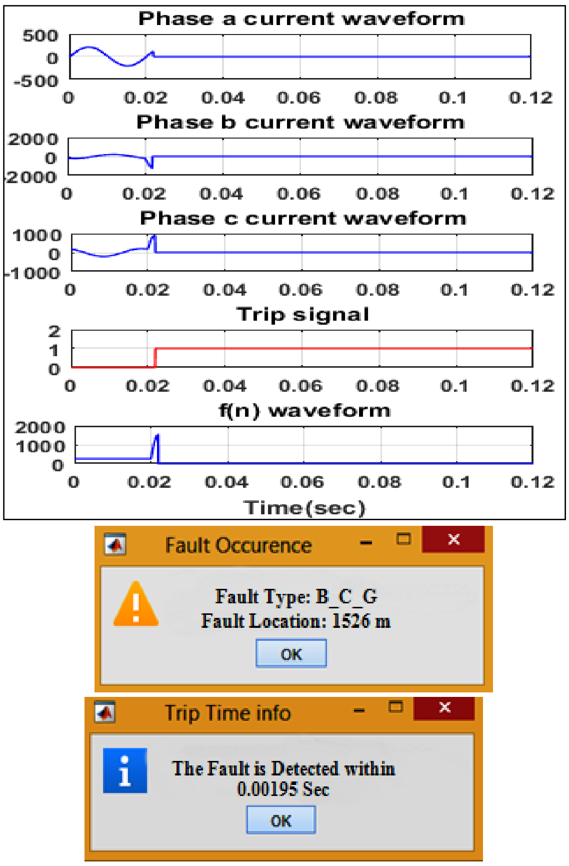

Fig. 31 B_C_G fault at L3

• *A_B Fault at L1*

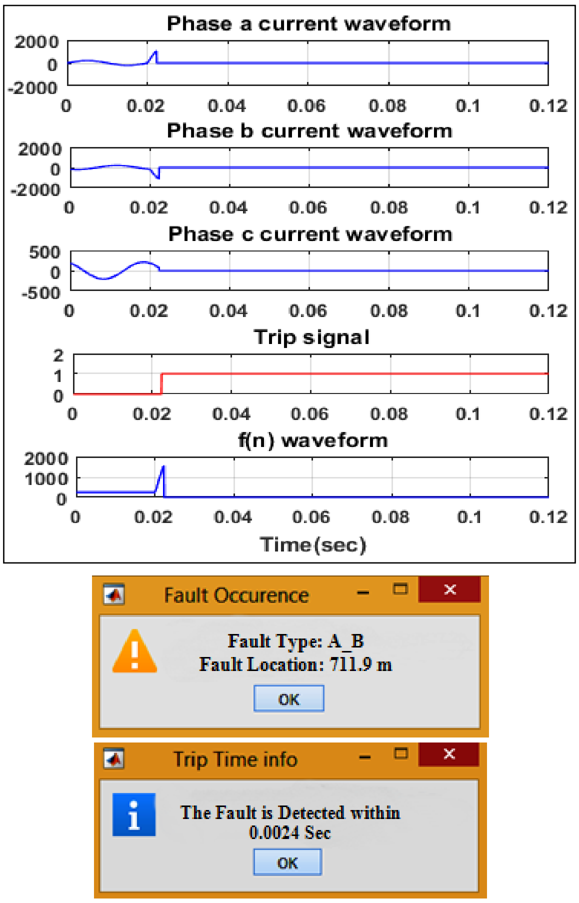

Fig. 32 A_B fault at L1

• *B_C Fault at L3*

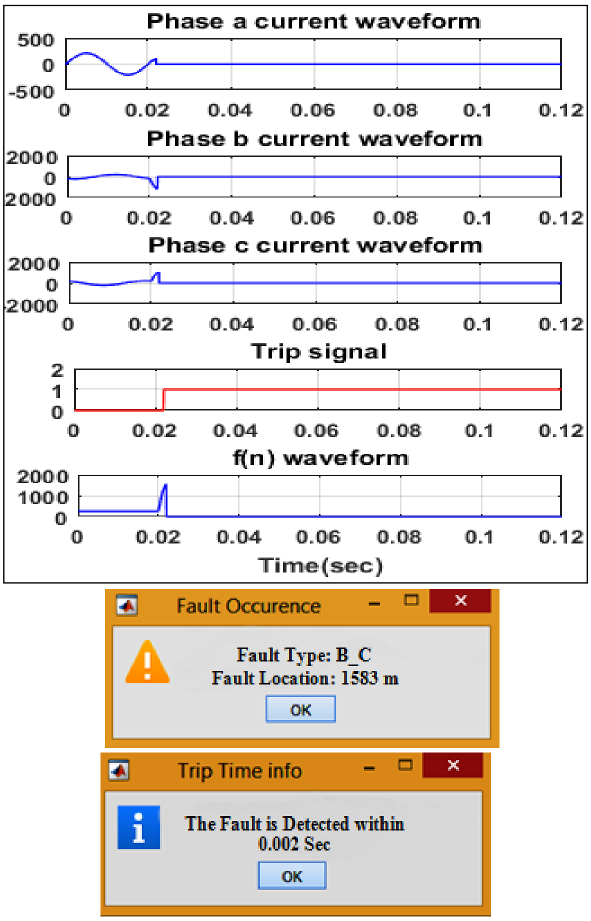

Fig. 34 B_C fault at L3

• *A_C Fault at L2*

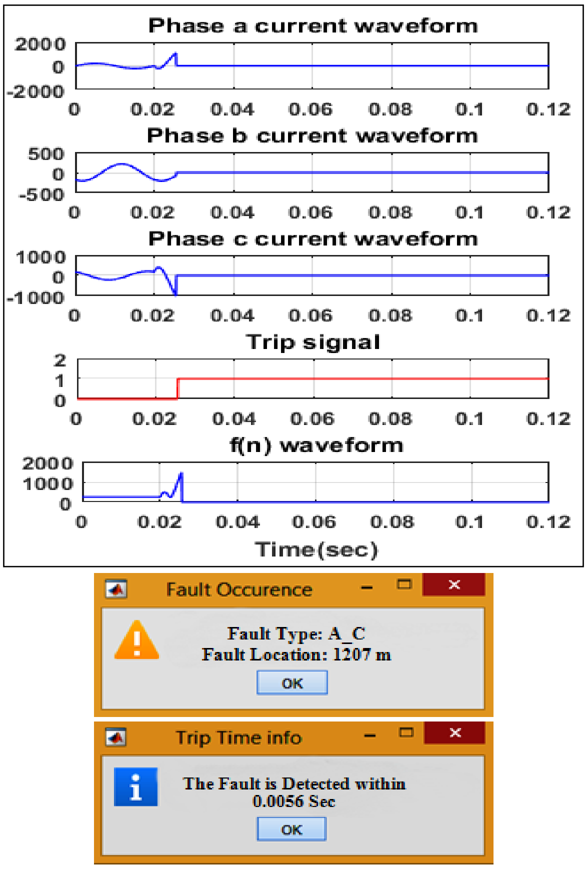

Fig. 33 A_C fault at L2

• *A_B_C Fault at L1*

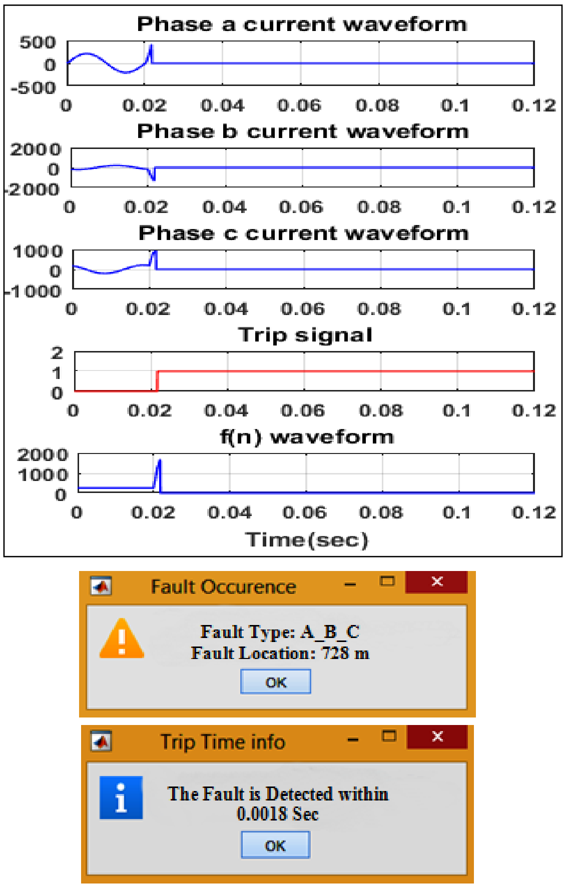

Fig. 35 A_B_C fault at L1

• *A_B_C Fault at L2*

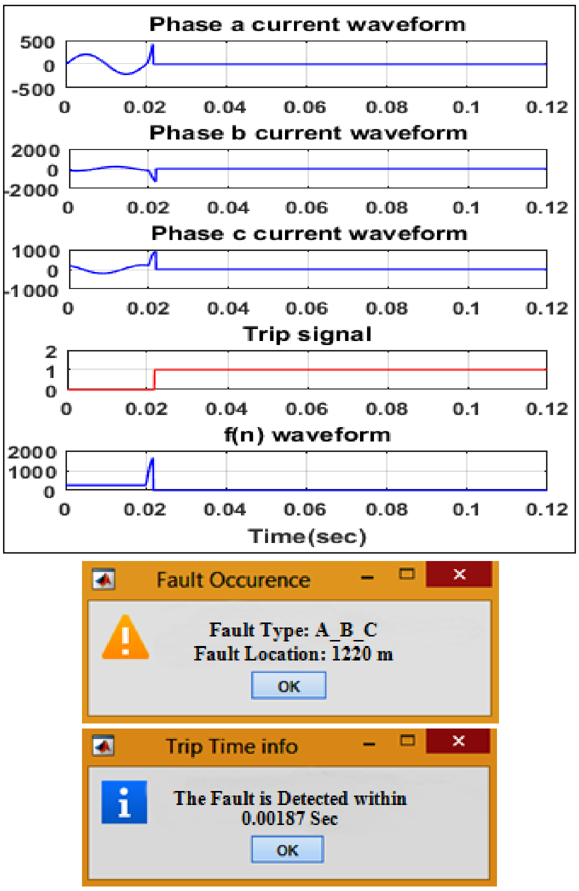

Fig. 36 A_B_C fault at L2

• *A_B_C Fault at L3*

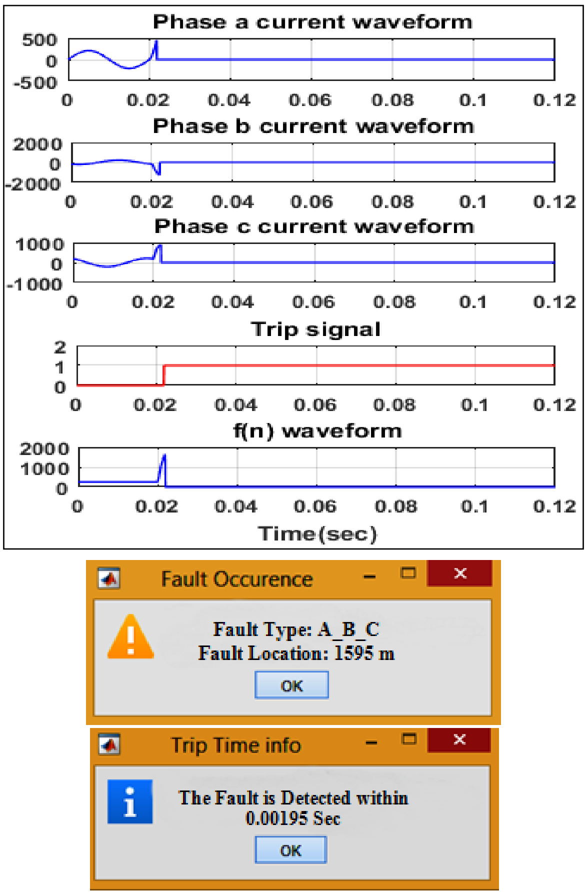

Fig. 37 A_B_C fault at L3

VII. Conclusions

Test results on the proposed Fault detection, classification and location schemes prove the following:

1) By utilizing the DWT, faults can successfully be detected, classified and localized utilizing only the first stage decompositions of the current samples by mother wavelet db2 related filters.
2) The Analysis of the function f[n] has proven its ability to detect faults accurately within small time intervals without the need for the three phase and zero sequence currents analysis that impose a lot of unnecessary processing in case of healthy states.
3) Since the energization of a capacitor bank or the main feeder associated transients has major effects on the detail coefficients of DWT decomposed current signals that can cause false indication of faults, The use of two thresholds in the detection phase results in better discrimination between healthy and faulty conditions.
4) The comparison between the two proposed fault type classification systems has led to the conclusion that utilizing an FIS can accurately classify single phase to ground and phase to phase faults, but can create false indications in some cases of phase to phase to ground and three phase faults; on the other hand the ANN proves to classify all fault types accurately.
5) The use of cascade forward neural networks shows good capability to classify and locate faults taking into account the complicated variation of DWT extracted current features with distance and fault resistances.
6) Two types of training functions has been tested for the cascade forward fault type and location networks. The trainlm function in most cases proves to have faster convergence and better test performance than the trainbr function. The results of the energy and RMS inputs tests has shown than the RMS input ANNs can converge in less number of epochs than the Energy input ones but can have less generality.
7) The energy representation of features is chosen for the proposed scheme while trainlm training function is chosen for all ANNs except for LLG and LL fault location ANNs.
8) The overall proposed scheme proves to have fast and secure functionality along with good fault information accuracy. As a result the dispatched maintenance crew can find the faulty type and section of feeder conductors in order to fix them and reduce outage time.

\

VIII. APPENDIX

Substation	**Source**	**Transformer T1**		
	33 kV	**Turns ratio**	33/11 kV	
		Type	YG-YG	
		Rating	10 MVA	
		R	0.002 p.u	
		X	0.08 p.u	
Conductor specifications	**Phase Conductor**		**Neutral Conductor**	
	Type	**Size**	**Type**	**Size**
	ACSR	336,400 26/7	ACSR	4/0 6/1
	Phase Inductance Matrix in H/km			
	0.0017768	0.0008269	0.0006344	
	0.0008269	0.0017277	0.0006982	
	0.0006344	0.0006982	0.0017555	
	Phase Resistance Matrix in Ω/km			
	0.28434	0.0969	0.09538	
	0.0969	0.2899	0.09817	
	0.09538	0.09817	0.28676	
Length	2 km			
Node 5 Load	160 kW, Unity P.F			
Node 10 Load	2 MW, Unity P.F			
Node 15 Load	500 kW, Unity P.F			
Node 20 Load	1000 kVA, 0.8 P.F			
Node 20 Capacitor bank	600 kVAr			
Distribution transformer T2,T3	**Turns ratio**	11/0.4 kV		
	Type	YG-YG		
	Rating	1 MVA		
	R	0.002 p.u		
	X	0.08 p.u		

REFERENCES

[1] M. A. Kafiey, “A Wavelet Packet Transform Based on-Line Technique for the Protection of Three-phase Interior Permanent Magnet Motors,” M.S. thesis, Memorial University of Newfoundland, St. John’s, Canada, May 2006.

[2] Suman Devi, Nagendra K. Swarnkar, Sheesh Ram Ola and Om Prakash Mahela, “Detection of Transmission Line Faults Using Discrete Wavelet Transform,” in Proc. 2016 Conference on Advances in Signal Processing (CASP),pp. 133-138.

[3] M. Jayabharata Reddy, D. K. Mohanta, “ A modular approach for classification and location of arcing and non-arcing faults on transmission lines,” Int. J. Energy Technology and Policy, vol. 7, no. 4, pp. 309-324, 2011.

[4] Majid Jamil, Rajveer Singh and Sanjeev Kumar Sharma, “Fault identification in electrical power distribution system using combined discrete wavelet transform and fuzzy logic,” Journal of Electrical Systems and Information Technology, vol. 2, pp. 257-267, 2015.

[5] A. Abdollahi and S. Seyedtabaii, “ Comparison of Fourier & Wavelet Transform Methods for Transmission Line Fault Classification,” in Proc. 2010 Power Engineering and Optimization Int. Conf., pp. 579-584.

[6] Binoy Saha, Bikash Patel, Parthasarathi Bera, “ DWT and BPNN Based Fault Detection, Classification and Estimation of Location of HVAC Transmission Line,” in Proc. 2016 Intelligent Control Power and Instrumentation (ICICPI) International Conference, pp. 174-178 .

[7] Sunil Singh and D. N. Vishwakarma, “ Application of DWT and ANN for Fault Classification and Location in a Series Compensated Transmission Line,” in Proc. Power Systems (ICPS), 2016 IEEE 6th International Conference, pp.1-6.

[8] Kapildev Lout and R. K. Aggrawal, “A Feedforward Artificial Neural Network Approach to Fault Classification and Location on a 132kV Transmission Line Using Current Signals Only,” in Proc. 2012 47th International Universities Power Engineering Conference (UPEC), pp. 1-6.

[9] Mamta Patel and R. N. Patel, “ Fault analysis in transmission lines using neural network and wavelets,” in Proc. 2015 Signal Processing and Integrated Networks (SPIN) Int. Conf., pp. 719-724.

[10] Behnam Feizifar, Mahmoud Reza Haghifam, Soodabeh Soleymani and Amirsam Jamilazari, “ Fault Location in Combined Overhead Line and Underground Cable Distribution Networks Using Fault Transient Based Mother Wavelets,” in Proc. 2013 Environment and Electrical Engineering Conf. (EEEIC) .

[11] Liqun Shang, Wensong Zhai and Pei Liu, “ Study of Fault Location in Transmission Line Using S Transform,” in Proc. 2016 Computer, Consumer and Control Conf. (IS3C), pp. 85-88.

[12] R. Das, M. S. Sachdev and T. S. Sidue, “ A Fault Locator for Radial Subtransmission and Distribution Lines,” IEEE Power Engineering Society Summer Meeting, vol. 1, pp. 443-448, 2000.

[13] Rahman Dashti, Mohammad Daisy and Hamid Reza Shaker, “A new Method presentation for locating Fault in Power Distribution Networks,” in Proc. 2016 Electrical Apparatus and Technologies International Symposium (SIELA), pp. 1-4.

[14] A. H. A. Bakar, M. S. Ali, ChiaKwang Tan, H. Mokhlis and H. Arof, H. A. Illias, “High impedance fault location in 11 kV underground distribution systems using wavelet transforms,” International Journal of Electrical Power & Energy Systems, vol. 55, pp. 723-730, 2014.

[15] H. Mokhlis and H. Y. Li, “Fault location estimation for distribution system using simulated voltage sags data,” in Proc. 2007 Universities Power Engineering Conf. (UPEC), pp. 242-247.

[16] S. Bunjongjit, A. Ngaopitakkul and C. Pothisarn, “A Discrete Wavelet Transform and Fuzzy Logic Algorithm for Identifying the Location of Fault in Underground Distribution System,” in Proc. 2013 Fuzzy Theory and Its Application (iFUZZY) Int. Conf., pp. 415-419.

[17] J. J. Mora, G. Garrillo and L. Pérez, “Fault Location in Power Distribution System using ANFIS Nets and Current Patterns,” in Proc. 2006 Transmission & Distribution Conference and Exposition, pp. 1-6.

[18] Md. Abdul Kalam, Majid Jamil and A. Q. Ansari, “Wavelet based ANN Approach for Fault Location on a Transmission Line,” in Proc. 2010 Power Electronics, Drives and Energy Systems (PEDES) & Power India Joint Int. Conf..

[19] A. Abdollahi and S. Seyedtabaii, “Transmission Line Fault Location Estimation by Fourier & Wavelet Transforms Using ANN,” in Proc. 2010 4th International Power Engineering and Optimization Conference (PEOCO), pp. 573-578.

[20] W. H. Kersting, Distribution System Modelling and Analysis, 1nd Edition, Boca Raton, Florida: CRC Press, 2002, p. 77-95.

[21] Distribution Test Feeder Working Group, (Aug. 2013). Distribution test feeders. IEEE PES Power & Energy Society. [Online]. Available:

https://www.ewh.ieee.org/soc/pes/dsacom/testfeeders/feeder123.zip.

[22] Rodrigo Hartstein Salim, Karen Rezende Caino De Oliveira and Arturo Suman Bretas, “Fault detection in primary distribution systems using wavelets,” in Proc. Power Systems Transients Int. Conf., France, June 2007.

[23] F. Martin, J. A. Aguado, M. Medina, and M. Munoz, “Classification of faults in double circuit lines using wavelet transforms,” 2008 IEEE Int. Conf. on Industrial Technology.

[24] A. I. Megahed, A. Monem Moussa, H. B. Alrefaie and Y. M. Marghany, “ Selection of a Suitable Mother Wavelet for Analyzing Power System Fault Transients,” in Proc. 2008 IEEE Power and Energy Society General Meeting, pp. 1-7.

[25] Habeeb J. Nekad and Mustafa M. Ibrahim,” Broken Bar Fault Detection based on the Discrete Wavelet Transform and Artificial Neural Network,” Asian Transactions on Engineering, vol. 3, Iss. 2, May 2013.